THE JOURNAL OF PHYSICAL CHEMISTRY LETTERS
A JOURNAL OF THE AMERICAN CHEMICAL SOCIETY

pubs.acs.org/JPCL Letter

From Solution to Surface: Persistence of the Diradical Character of a Diindenoanthracene Derivative on a Metallic Substrate

Jeremy Hieulle,* Carlos Garcia Fernandez, Niklas Friedrich, Alessio Vegliante, Sofia Sanz, Daniel Sánchez-Portal, Michael M. Haley, Juan Casado, Thomas Frederiksen, and José Ignacio Pascual*

Cite This: J. Phys. Chem. Lett. 2023, 14, 11506−11512 Read Online

ACCESS | Metrics & More | Article Recommendations | Supporting Information

ABSTRACT: Organic diradicals are envisioned as elementary building blocks for designing a new generation of spintronic devices and have been used in constructing prototypical field effect transistors and nonlinear optical devices. Open-shell systems, however, are also reactive, thus requiring design strategies to "protect" their radical character from the environment, especially when they are embedded in solid-state devices. Here, we report the persistence on a metallic surface of the diradical character of a diindeno[*b*,*i*]anthracene (DIAn) core protected by bulky end-groups. Our scanning tunneling spectroscopy measurements on single-molecules detected singlet−triplet excitations that were absent for DIAn species packed in assembled structures. Density functional theory simulations unravel that the molecular geometry on the metal substrate can crucially modify the value of the singlet−triplet gap via the delocalization of the radical sites. The persistence of the diradical character over metallic substrates is a promising finding for integrating radical-based materials into functional devices.

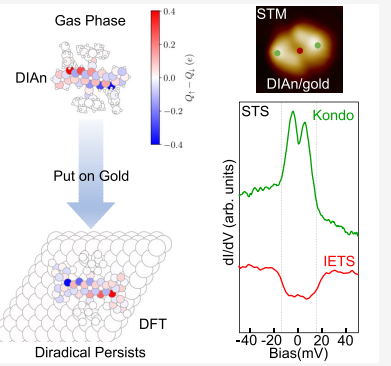

Diradical molecules are promising candidates for the design of new-generation nonlinear optic (NLO)[1] and spintronic devices.[2,3] As examples, diradicals have been used to build spin filters[4] and field-effect transistors,[5] and they could potentially be used for memory storage devices.[1,3] In recent years, much focus has been directed to the understanding of the interactions established between the two spin centers of a diradical and how those interactions can be controlled.[1,6−8]

To date, the impact of a contact metal electrode on the electronic and magnetic properties of diradicals remains unclear, especially because the influence of molecular geometry, adsorption, and packing has yet to be revealed. Those parameters have been shown to play a crucial role in defining the magnetic properties of metal−organic molecules on surfaces[9−14] and are also expected to affect the properties of purely organic diradicals. Most of the recent studies on diradicals have been performed in soft solution or solid environments. Therefore, exploring their structures on metallic surfaces can be of great significance to disentangle the remaining unknown questions about these fascinating molecules.

Among all diradical molecules, the diindeno[*b*,*i*]anthracene (DIAn) framework is of particular interest due to its high solubility in common organic solvents, high thermal stability, ease of sublimation, and excellent oxidation resistance.[15] DIAn has also exceptional electronic properties, such as a small singlet−triplet gap and a balanced ambipolar charge-transport behavior.[16−19] Owing to these properties, DIAn molecules are perfectly suitable for mass production for future market applications in, for instance, high-performance organic field-effect transistors.[5] In a more fundamental scenario, DIAn is ideally suited to investigate, at the atomic scale, the magnetic behavior of prototypical diradical molecules in contact with inorganic interfaces, seeking strategies to maintain their molecular functionality when they form part of solid state devices.

Here we demonstrate that individual DIAn molecules maintain their diradical character on a metallic substrate with a reduced singlet−triplet gap compared to values observed in the solid state. We studied DIAn molecules and assemblies adsorbed on an atomically clean Au(111) substrate and probed inter- and intramolecular spin interactions by scanning tunneling spectroscopy (STS). Using the Kondo effect as a fingerprint of molecular magnetism,[20−26] we probe local spin interactions inside the diradicals, unraveling underlying mechanisms at the origin of magnetic interactions between the two spin centers of the diradical. More importantly, we demonstrate that those magnetic interactions depend on the molecular conformation over the surface and on their interaction with other species in assembled nanostructures. In particular, supported by density functional theory (DFT) simulations, we show that the rotation of mesityl substituents

Received: August 28, 2023
Revised: October 27, 2023
Accepted: October 27, 2023
Published: December 13, 2023

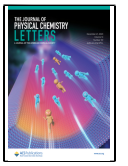

https://doi.org/10.1021/acs.jpclett.3c02401
J. Phys. Chem. Lett. 2023, 14, 11506−11512

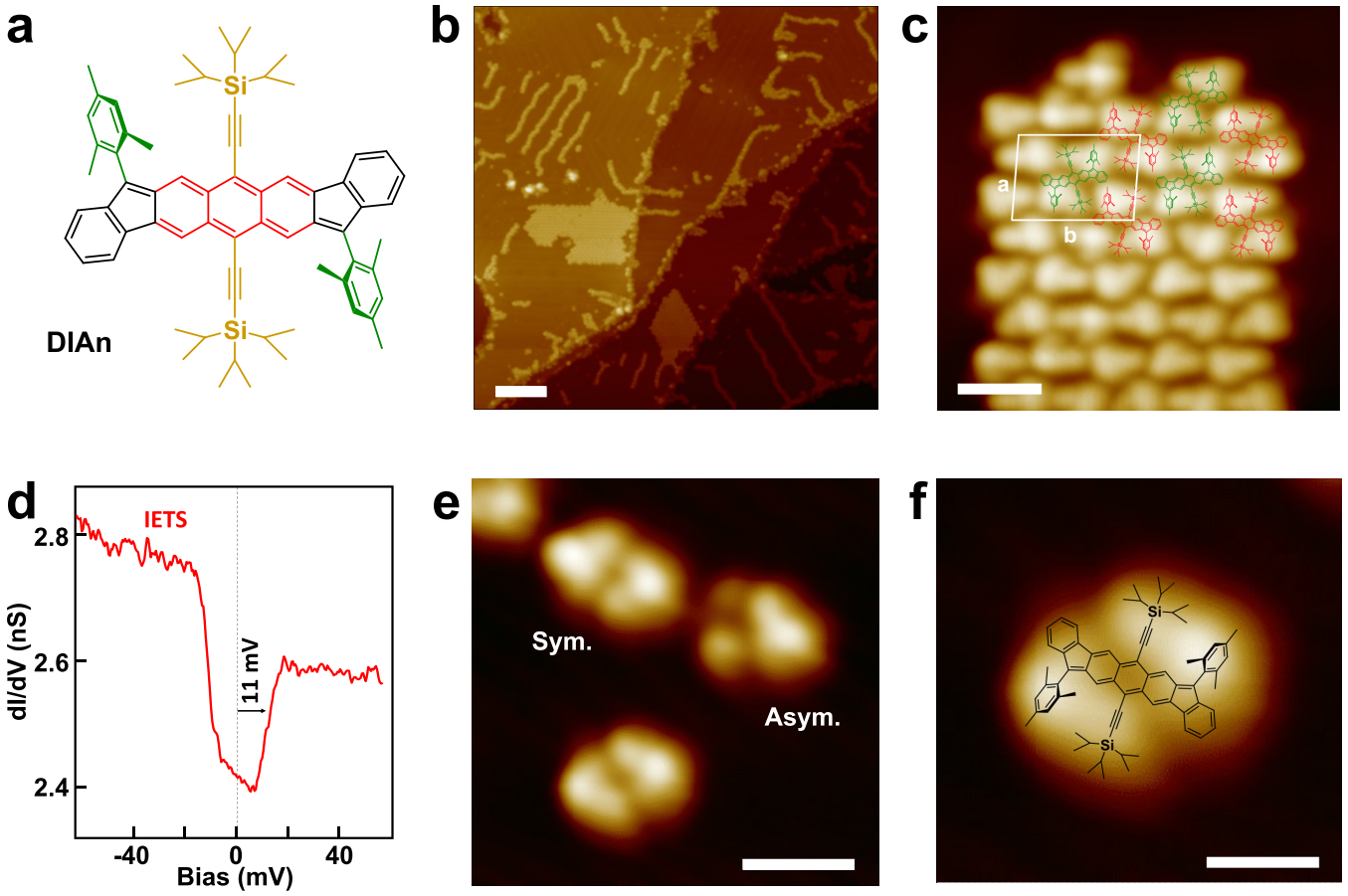

Figure 1. Molecular packing of DIAn diradicals on Au(111). (a) Chemical structure of DIAn. The anthracene core is highlighted in red, while the (triisopropylsilyl)ethynyl groups and mesityl groups are highlighted in orange and green, respectively. Indene groups are drawn in black. (b) STM image showing the typical molecular chains and close-packed domains formed by DIAn. (c) STM image of the close-packed domain. A model of the molecular packing indicating the bimolecular unit cell is superimposed on the topographic image. (d) dI/dV spectra obtained at the anthracene core of a single diradical molecule in the domain, showing a vibrational inelastic electron tunneling (IETS) feature. (e, f) Topographic images of isolated DIAn monomer obtained by lateral manipulation with the STM tip. Scale bars: (b) 20 nm; (c−e) 2 nm; (f) 1 nm.

modifies the magnetic interaction between the two spin centers of a single DIAn molecule. These results outline the relevance of intermolecular interactions in supramolecular nanoarchitectures in the magnetic properties of open-shell molecular systems.

The core of the DIAn molecule is composed of two indene groups (black section, Figure 1a), spaced by an anthracene bridge (red section, Figure 1a). The indene moieties endow DIAn with the radical character of the molecule[15] and, here, incorporate bulky mesityl substituents (green section in Figure 1a) for protecting them. Additionally, (triisopropylsilyl)ethynyl groups (CCSi(i-Pr)$_3$, orange section, Figure 1a) are attached to the quinoidal anthracene core to provide high stability against oxidation and high solubility. Details of the synthesis of DIAn have been reported previously.[15]

We deposited DIAn diradicals onto an atomically flat Au(111) surface by thermal sublimation of the molecular powder in ultrahigh vacuum at a temperature of 563 K. Scanning tunneling microscopy (STM) images at 4 K show that DIAn diradicals assemble in two types of structures for submonolayer coverages: extended close-packed domains and molecular chains (Figure 1b). The former consists of a parallelogram network with a unit cell (white box in Figure 1c) containing two DIAn molecules, as indicated in the molecular model in Figure 1c. Differential conductance (dI/dV) spectra on the molecules in these close-packed domains show two bias-symmetric steps at ±11 meV (Figure 1d). The spectral feature is highly localized at the central anthracene core and absent over the protruding groups. We tentatively attribute it to the inelastic excitation of a molecular vibrational mode.[27,28] In fact, Raman spectra of DIAn crystals show a prominent band around 11 meV corresponding to the out-of-phane deformation of the mesityl and of the isopropylsilyl groups (Figures S1 and S2). Molecular chains, in contrast to the domains, are rather disordered structures, weakly packed and oriented along the Au(111) herringbone reconstruction.

To explore single DIAn diradicals, we moved apart individual molecules from the chain structures using the tip of the STM. As in the domains, DIAn molecules appear in STM images as two inverted protrusions, each composed of the bulkier mesityl groups (Mes) and the lower (triisopropylsilyl)ethynyl moiety (CCSi(i-Pr)$_3$), as shown in Figures 1e,f. It is important to note that in some occasions tip-manipulated DIAn molecules appeared with an asymmetric configuration, with one-half appearing with a lower height (top right of Figure 1e). Although we cannot state the precise origin of this different aspect, we speculate that it might be due to a distortion (e.g., a rotation) of the mesityl groups.

The open-shell character of the isolated DIAn species could be resolved via STS measurements. Differential conductance

https://doi.org/10.1021/acs.jpclett.3c02401
J. Phys. Chem. Lett. 2023, 14, 11506−11512

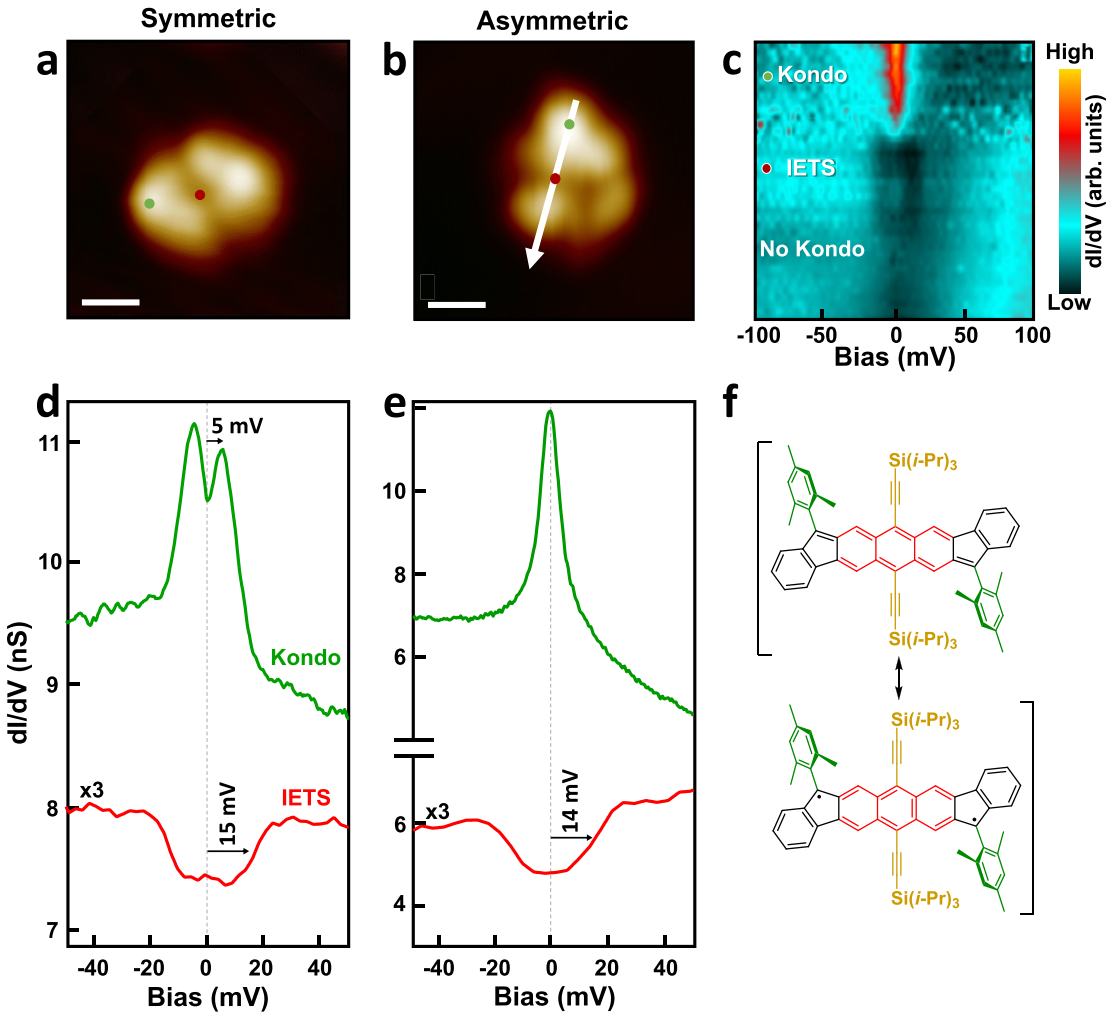

Figure 2. Magnetic fingerprints of isolated DIAn diradical molecule. (a, b) Topographic images of the symmetric and asymmetric DIAn diradical. Scale bar corresponds to 1 nm. Colored circles in the topographic image mark the positions where dI/dV spectra were recorded. The corresponding dI/dV spectra measured on symmetric and asymmetric DIAn diradical are plotted in (d) and (e), respectively. A split Kondo feature is observed at the mesityl groups (Mes), confirming the diradical character of the symmetric DIAn molecule, whereas a single Kondo peak is observed for the asymmetric DIAn molecule (green curves). In both cases, a vibrational inelastic electron tunneling (IETS) feature is observed on the central anthracene core of the molecule. The signal amplitude of the IETS spectra was multiplied by three for a better reading (red curves). (c) dI/dV stacked plot taken along the white arrow in (b), showing that the Kondo is located on the mesityl group of the molecule while the vibrational IETS feature is found at the anthracene position (red). The Kondo appears at only one side of the asymmetric molecule, on its brighter mesityl group. (f) Non-Kekulé resonance diradical structure of DIAn, showing that the two radicals are located at the junction between the indene (black) and mesityl (green) groups of the molecule.

(dI/dV) spectra over their mesityl groups (Figure 2a) resolved now two narrow peaks centered symmetrically around zero bias (green curve in Figure 2d), which reveal the survival of their diradical state on the Au(111) substrate. Owing to a weak interaction of the radical state with the metal surface, its associated spin $S = 1/2$ can be partially screened via the Kondo effect,[10,20,29−31] resulting in a narrow logarithmic resonance at zero bias. However, over DIAn's bulky sides, we observed, instead, a double-peak structure. This is attributed to the presence of two antiferromagnetically interacting radical states. As shown in Figure 2f, DIAn can lie either in an open shell non-Kekulé structure or in a closed shell state. In the former, two radicals appear localized at the junctions between the indene and mesityl groups (i.e., at the apical carbons of the five-membered rings), spaced by the central anthracene bridge, which mediates their antiferromagnetic interaction J between them, forming a singlet ground state. In this configuration, the lower dI/dV signal at zero-bias reflects the absence of Kondo states for the singlet ground state. At tunneling energies equal to or larger than J, dI/dV peaks reflect the excitation of a triplet state, with their corresponding energy providing a direct measure of J.[22,32] Above these onsets, Kondo-like dynamical fluctuations in the triplet state, now accessible by inelastic tunneling electrons, result in the logarithmic tail and the appearance of a split-Kondo resonance rather than inelastic steps.[33,34]

In contrast, on the distorted DIAn molecules, a single dI/dV peak centered at zero bias is measured only over the brighter mesityl group (green curve, Figure 2e), while a featureless spectrum appears on the lower half of the molecule (dI/dV stacked plot, Figure 2c). This reveals that on the *distorted* side, the radical state is either quenched probably due to a conformational change or a strong interaction with the metal underneath. Additionally, bias-symmetric dI/dV steps at ±15

https://doi.org/10.1021/acs.jpclett.3c02401
J. Phys. Chem. Lett. 2023, 14, 11506−11512

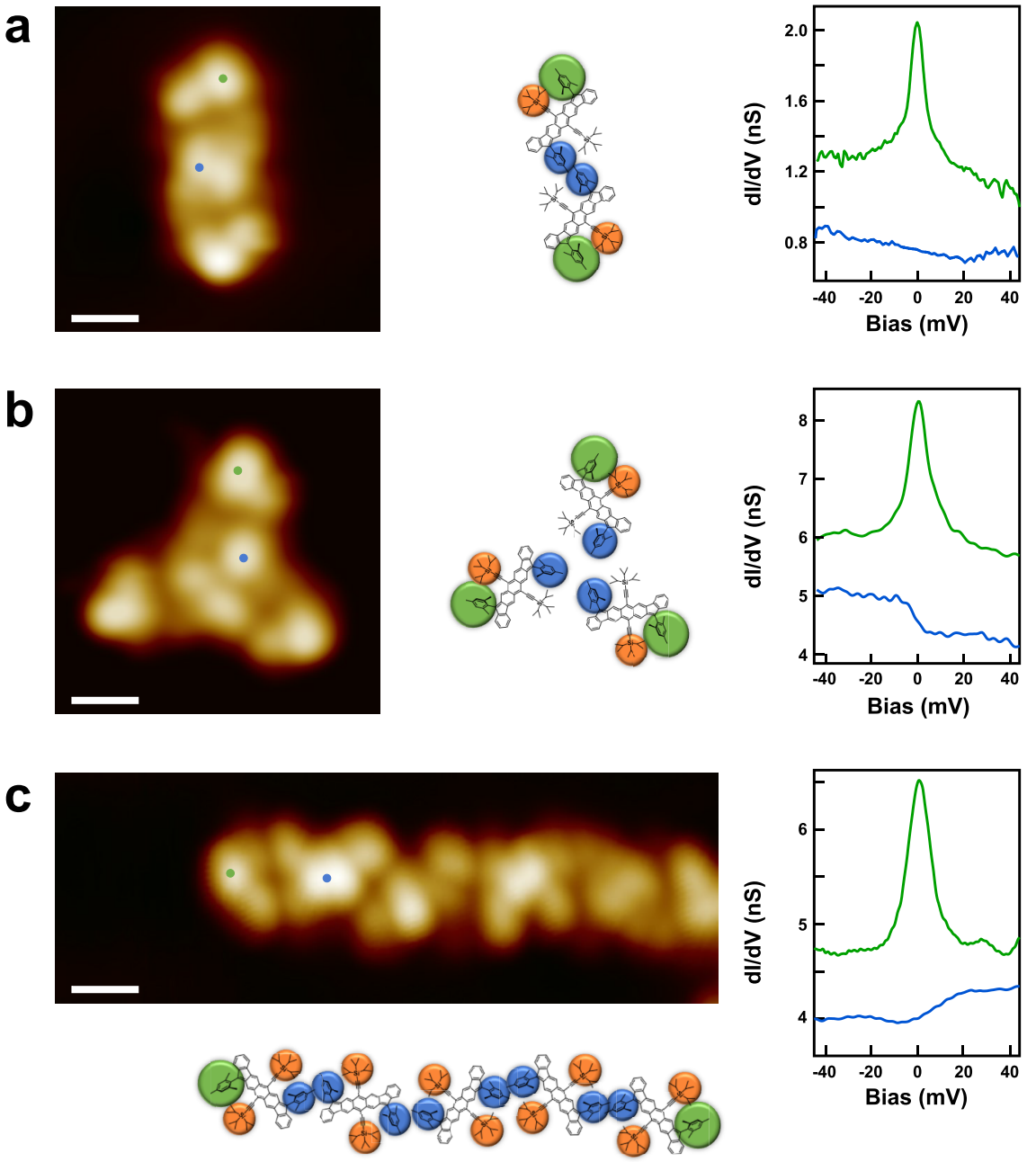

Figure 3. Kondo feature in nanostructures made of a few DIAn molecules. STM images showing close-packed nanostructures made of several DIAn molecules, with the corresponding chemical structures and characteristic dI/dV spectra taken over the regions highlighted in green and blue in the chemical models. The data were obtained for (a) dimer, (b) trimer, and (c) molecular chain of DIAn molecules. Evident Kondo features are observed on specific positions of the nanostructures. Color code: strongly interacting mesityl group (blue), noninteracting mesityl group (green), and (triisopropylsilyl)ethynyl group (orange). Scale bars in (a−c) correspond to 1 nm.

meV were detected over the central anthracene core on both pristine and distorted DIAn species (red curves in Figure 2d,e). Because we observe them with similar intensity on the diradical and monoradical species, we can safely exclude their magnetic origin. Instead, we tentatively assign them to the excitation of the vibrational mode observed on the assembled domains, here at slightly higher energy, probably due to the different conformations adopted when isolated on the metal substrate.

The shifted Kondo resonances on DIAn molecules amount to a singlet−triplet excitation energy of $E_{ST} \simeq 5$ meV. This value is significantly smaller than the singlet−triplet energy difference obtained from density functional theory simulations of DIAn in the gas phase.[15] In particular, our DFT results in Figures S3a and S3b corroborate the singlet ground state and find a parallel spin configuration at almost 140 meV above, signaling for a singlet−triplet gap E_{ST} much larger than in our experiment, and similar to previous measurements of DIAn.[17]

The origin of the smaller inter-radical exchange interaction observed in the experiment is likely connected with molecular modifications when adsorbed onto the gold surface. We have simulated the geometric relaxation and magnetic state of a DIAn molecule on a Au(111) slab using DFT (results summarized in Figures S3−S7). The first important result is that DFT reproduces the survival of the diradical character of

https://doi.org/10.1021/acs.jpclett.3c02401
J. Phys. Chem. Lett. 2023, 14, 11506−11512

DIAn molecules on the gold surface (Figure S3g). The molecule is physisorbed and maintains C−Au distances larger than 3 Å. After geometry optimizations, two magnetic configurations were converged corresponding to a $S = 0$ ground state and an $S = 1$ ($2\mu_B$) excited state, with an energy spacing significantly smaller than in the gas phase. Thus, DFT confirms that on the gold surface, the exchange interaction between indene radicals is reduced. The metallic substrate imposes, first, a partial planarization on the molecular structure by rotating the mesityl groups (Mes) toward the diindeno anthracene plane. As shown in Figure S4, the mesityl rotation induces a slight delocalization of the radical toward their aromatic center, which effectively increases the separation between spin centers and, consequently, reduces their magnetic interaction. Additional corrections to the simulations due to Coulomb correlations (considered in Figure S6) or the renormalization of exchange coupling due to Kondo correlations[35] can account for the further reduction of the reduced exchange observed in our experiments.

Our findings demonstrate that the commonly assumed inert role of molecular substituents[15] (e.g., Mes, CCSi(i-Pr)$_3$) on the active magnetic properties of diindeno[b,i]anthracene derivatives needs to be revised when the diradicals are put in contact with a metallic electrode. Although, unpaired electron spins remain present in the molecule, their interaction is altered significantly upon adsorption on a metallic electrode. We found that the CCSi(i-Pr)$_3$ group connected at the anthracene core allows preserving the spin polarization of isolated DIAn diradicals on gold. Figure S7 shows that when the two CCSi(i-Pr)$_3$ groups were replaced by CCSiMe$_3$, DIAn molecules are found to adsorb closer to the surface. In that case, the gold substrate imposes a bending of CCSi(i-Pr)$_3$ triple bonds (Figures S7a−c), while a gold atom is slightly pushed up from the surface plane (Figure S7a). Such a modification of the molecule−substrate separation modifies the charge distribution and quenches spin polarization over the molecular backbone.

Next, we show that the spin interaction in DIAn diradicals is modified in close-packed nanostructures made of a few molecules. Figure 3 shows nanostructures formed by two, three, or more DIAn molecules. Spectra recorded on the interacting mesityl groups of a DIAn dimer (Figure 3a, blue dot) reveal the absence of a magnetic fingerprint (blue curves), while spectra on the noninteracting mesityl groups (green dot) reveal now a single Kondo feature (green curves). This is further confirmed by spatial maps of the Kondo resonance shown in Figure S8, which illustrate the localization of the Kondo signal exclusively over external mesityl termini. This observation is consistent across other interacting molecular nanostructures such as trimers (Figure 3b) and molecular chains (Figure 3c).

The absence of a Kondo resonance on the neighboring mesityls can be explained caused as a combination of both a finite overlap of their electronic wave function of two neighboring spins and the concomitant intramolecular rotation of the involved mesityl groups for the assembly. Nevertheless, the quenching of one of the two radicals of DIAn also explains the observation of a single Kondo resonance on the external mesityl groups in DIAn dimers, trimers, and chains, in clear contrast with the split Kondo feature observed in isolated molecules. This observation also explains the complete quenching of all Kondo signals in extended 2D close-packed domains, as shown earlier (Figure 1).

In conclusion, here, we report the survival of the magnetic state of DIAn diradicals upon their adsorption on a Au(111) surface. We studied the spin interactions in the molecule through the many-body Kondo effect by performing scanning tunneling spectroscopy measurements and density functional theory calculations. The significant results from this study are (1) the persistence of the diradical singlet ground state upon adsorption, (2) the detection of spin interactions between the two spin centers of a single diradical, (3) the control over intermolecular spin interactions through the formation of nanostructures by self-assembly or STM tip manipulation, and (4) the demonstration of the substrate influence on the lowering of the singlet−triplet gap of the DIAn diradical by imposing a rotation of its mesityl groups. Importantly, these are crucial questions raised that need to be solved for the future use of diradicals in spintronic and NLO devices in which the molecules are in contact with metal electrodes. Our study paves the way to this by precise control of the spin interactions in isolated molecules and assembled nanostructures made of diradicals.

■ ASSOCIATED CONTENT

Supporting Information

The Supporting Information is available free of charge at https://pubs.acs.org/doi/10.1021/acs.jpclett.3c02401.

Section A: vibrational mode of DIAn; Section B: energy calculation of singlet−triplet states in DIAn adsorbed on gold; Section C: change in electronic structure after rotation of mesityl groups; Section D: projected density of states and bond order modification in the gas phase; Section E: influence of Coulomb repulsion U in the HOMO−LUMO gap, singlet−triplet energy and bond lengths; Section F: influence of substituent chemical composition on the magnetic properties of the DIAn molecule; Section G: Kondo map of DIAn trimers; Section H: controlling the Kondo signature by lateral manipulation; Section I: comparison of the long-range spectra of molecular chains and domains; Section J: correlation between molecular orbital positions and Kondo resonance; Section K: methods (PDF)

■ AUTHOR INFORMATION

Corresponding Authors

Jeremy Hieulle − *CIC nanoGUNE-BRTA, 20018 Donostia-San Sebastián, Spain;* orcid.org/0000-0003-4891-4007; Email: jeremy.hieulle@uni.lu

José Ignacio Pascual − *CIC nanoGUNE-BRTA, 20018 Donostia-San Sebastián, Spain; Ikerbasque, Basque Foundation for Science, 48013 Bilbao, Spain;* Email: ji.pascual@nanogune.eu

Authors

Carlos Garcia Fernandez − *Donostia International Physics Center (DIPC), 20018 Donostia-San Sebastián, Spain*

Niklas Friedrich − *CIC nanoGUNE-BRTA, 20018 Donostia-San Sebastián, Spain;* orcid.org/0000-0001-5353-5680

Alessio Vegliante − *CIC nanoGUNE-BRTA, 20018 Donostia-San Sebastián, Spain*

Sofia Sanz − *Donostia International Physics Center (DIPC), 20018 Donostia-San Sebastián, Spain;* orcid.org/0000-0002-2792-2721

https://doi.org/10.1021/acs.jpclett.3c02401
J. Phys. Chem. Lett. 2023, 14, 11506−11512

Daniel Sánchez-Portal − *Donostia International Physics Center (DIPC), 20018 Donostia-San Sebastián, Spain; Centro de Física de Materiales MPC (CSIC/UPV-EHU), 20018 Donostia-San Sebastián, Spain;* orcid.org/0000-0001-6860-8790

Michael M. Haley − *Department of Chemistry & Biochemistry and the Materials Science Institute, University of Oregon, Eugene, Oregon 97403-1253, United States;* orcid.org/0000-0002-7027-4141

Juan Casado − *Department of Physical Chemistry, University of Malaga, 229071 Malaga, Spain;* orcid.org/0000-0003-0373-1303

Thomas Frederiksen − *Donostia International Physics Center (DIPC), 20018 Donostia-San Sebastián, Spain; Ikerbasque, Basque Foundation for Science, 48013 Bilbao, Spain;* orcid.org/0000-0001-7523-7641

Complete contact information is available at: https://pubs.acs.org/10.1021/acs.jpclett.3c02401

Notes

The authors declare no competing financial interest.

■ ACKNOWLEDGMENTS

We gratefully acknowledge financial support from Spanish MCIN/AEI/10.13039/501100011033 and the European Regional Development Fund (ERDF) through Grants PID2019-107338RBC61, PID2020-115406GB-I00, PID2021-127127NB-I00, and CEX2020-001038-M and from the European Union (EU) through Horizon 2020 (FET-Open project SPRING Grant 863098). J.C. also acknowledges the Junta de Andalucía, Spain (PROYEXCEL-0328), and M.M.H. acknowledges the NSF (CHE-1954389) for financial support.

■ REFERENCES

(1) Fukuda, K.; Nagami, T.; Fujiyoshi, J.-y.; Nakano, M. Interplay between Open-Shell Character, Aromaticity, and Second Hyperpolarizabilities in Indenofluorenes. *J. Phys. Chem. A* **2015**, *119*, 10620−10627.

(2) Shil, S.; Bhattacharya, D.; Misra, A.; Klein, D. J. A high-spin organic diradical as a spin filter. *Phys. Chem. Chem. Phys.* **2015**, *17*, 23378−23383.

(3) Tagami, K.; Tsukada, M. Spintronic Transport through Polyphenoxyl Radical Molecules. *J. Phys. Chem. B* **2004**, *108*, 6441−6444.

(4) Shil, S.; Bhattacharya, D.; Misra, A.; Klein, D. J. A high-spin organic diradical as a spin filter. *Phys. Chem. Chem. Phys.* **2015**, *17*, 23378−23383.

(5) Zong, C.; Yang, S.; Sun, Y.; Zhang, L.; Hu, J.; Hu, W.; Li, R.; Sun, Z. Isomeric dibenzooctazethrene diradicals for high-performance air-stable organic field-effect transistors. *Chem. Sci.* **2022**, *13*, 11442−11447.

(6) Rajca, A.; Takahashi, M.; Pink, M.; Spagnol, G.; Rajca, S. Conformationally Constrained, Stable, Triplet Ground State (S = 1) Nitroxide Diradicals. Antiferromagnetic Chains of S = 1 Diradicals. *J. Am. Chem. Soc.* **2007**, *129*, 10159−10170.

(7) Majzik, Z.; Pavliček, N.; Vilas-Varela, M.; Pérez, D.; Moll, N.; Guitián, E.; Meyer, G.; Peña, D.; Gross, L. Studying an antiaromatic polycyclic hydrocarbon adsorbed on different surfaces. *Nat. Commun.* **2018**, *9*, 1198.

(8) Karafiloglou, P. The double (or dynamic) spin polarization in π diradicals. *J. Chem. Educ.* **1989**, *66*, 816.

(9) Saiful, I.; Inose, T.; Tanaka, D.; Mishra, P.; Ogawa, T.; Komeda, T. Hybridized Kondo State Formed by π Radical Assemblies. *J. Phys. Chem. C* **2020**, *124*, 12024−12029.

(10) Zhang, Q.; Kuang, G.; Pang, R.; Shi, X.; Lin, N. Switching Molecular Kondo Effect via Supramolecular Interaction. *ACS Nano* **2015**, *9*, 12521−12528.

(11) Amokrane, A.; Klyatskaya, S.; Boero, M.; Ruben, M.; Bucher, J.-P. Role of π-Radicals in the Spin Connectivity of Clusters and Networks of Tb Double-Decker Single Molecule Magnets. *ACS Nano* **2017**, *11*, 10750−10760.

(12) Karan, S.; et al. Spin Manipulation by Creation of Single-Molecule Radical Cations. *Phys. Rev. Lett.* **2016**, *116*, 027201.

(13) Sánchez-Grande, A.; et al. Diradical Organic One-Dimensional Polymers Synthesized on a Metallic Surface. *Angew. Chem., Int. Ed.* **2020**, *59*, 17594−17599.

(14) DiLullo, A.; Chang, S.-H.; Baadji, N.; Clark, K.; Klöckner, J.-P.; Prosenc, M.-H.; Sanvito, S.; Wiesendanger, R.; Hoffmann, G.; Hla, S.-W. Molecular Kondo Chain. *Nano Lett.* **2012**, *12*, 3174−3179.

(15) Rudebusch, G. E.; Zafra, J. L.; Jorner, K.; Fukuda, K.; Marshall, J. L.; Arrechea-Marcos, I.; Espejo, G. L.; Ponce Ortiz, R.; Gómez-García, C. J.; Zakharov, L. N.; Nakano, M.; Ottosson, H.; Casado, J.; Haley, M. M. Diindeno-fusion of an anthracene as a design strategy for stable organic biradicals. *Nat. Chem.* **2016**, *8*, 753−759.

(16) Rudebusch, G. E.; Espejo, G. L.; Zafra, J. L.; Peña-Alvarez, M.; Spisak, S. N.; Fukuda, K.; Wei, Z.; Nakano, M.; Petrukhina, M. A.; Casado, J.; Haley, M. M. A Biradical Balancing Act: Redox Amphoterism in a Diindenoanthracene Derivative Results from Quinoidal Acceptor and Aromatic Donor Motifs. *J. Am. Chem. Soc.* **2016**, *138*, 12648−12654.

(17) Dressler, J. J.; Teraoka, M.; Espejo, G. L.; Kishi, R.; Takamuku, S.; Gómez-García, C. J.; Zakharov, L. N.; Nakano, M.; Casado, J.; Haley, M. M. Thiophene and its sulfur inhibit indenoindenodibenzothiophene diradicals from low-energy lying thermal triplets. *Nat. Chem.* **2018**, *10*, 1134−1140.

(18) Dressler, J. J.; Cárdenas Valdivia, A.; Kishi, R.; Rudebusch, G. E.; Ventura, A. M.; Chastain, B. E.; Gómez-García, C. J.; Zakharov, L. N.; Nakano, M.; Casado, J.; Haley, M. M. Diindenoanthracene Diradicaloids Enable Rational, Incremental Tuning of Their Singlet-Triplet Energy Gaps. *Chem.* **2020**, *6*, 1353−1368.

(19) Hayashi, H.; Barker, J. E.; Cárdenas Valdivia, A.; Kishi, R.; MacMillan, S. N.; Gómez-García, C. J.; Miyauchi, H.; Nakamura, Y.; Nakano, M.; Kato, S.-i.; Haley, M. M.; Casado, J. Monoradicals and Diradicals of Dibenzofluoreno[3,2-b]fluorene Isomers: Mechanisms of Electronic Delocalization. *J. Am. Chem. Soc.* **2020**, *142*, 20444−20455.

(20) Ternes, M.; Heinrich, A. J.; Schneider, W.-D. Spectroscopic manifestations of the Kondo effect on single adatoms. *J. Phys.: Condens. Matter* **2009**, *21*, 053001.

(21) Fernández-Torrente, I.; Franke, K. J.; Pascual, J. I. Vibrational Kondo Effect in Pure Organic Charge-Transfer Assemblies. *Phys. Rev. Lett.* **2008**, *101*, 217203.

(22) Li, J.; Sanz, S.; Corso, M.; Choi, D. J.; Peña, D.; Frederiksen, T.; Pascual, J. I. Single spin localization and manipulation in graphene open-shell nanostructures. *Nat. Commun.* **2019**, *10*, 200.

(23) Li, J.; Sanz, S.; Castro-Esteban, J.; Vilas-Varela, M.; Friedrich, N.; Frederiksen, T.; Peña, D.; Pascual, J. I. Uncovering the Triplet Ground State of Triangular Graphene Nanoflakes Engineered with Atomic Precision on a Metal Surface. *Phys. Rev. Lett.* **2020**, *124*, 177201.

(24) Wang, T.; Sanz, S.; Castro-Esteban, J.; Lawrence, J.; Berdonces-Layunta, A.; Mohammed, M. S. G.; Vilas-Varela, M.; Corso, M.; Peña, D.; Frederiksen, T.; de Oteyza, D. G. Magnetic Interactions Between Radical Pairs in Chiral Graphene Nanoribbons. *Nano Lett.* **2022**, *22*, 164−171.

(25) Turco, E.; Bernhardt, A.; Krane, N.; Valenta, L.; Fasel, R.; Juríček, M.; Ruffieux, P. Observation of the Magnetic Ground State of the Two Smallest Triangular Nanographenes. *JACS Au* **2023**, *3*, 1358−1364.

(26) Vilas-Varela, M.; et al. On-Surface Synthesis and Characterization of a High-Spin Aza-[5]-Triangulene. *Angew. Chem., Int. Ed.* **2023**, *62*, e202307884.

(27) Stipe, B. C.; Rezaei, M. A.; Ho, W. Single-Molecule Vibrational Spectroscopy and Microscopy. *Science* **1998**, *280*, 1732−1735.
(28) Bachellier, N.; Verlhac, B.; Garnier, L.; Zaldívar, J.; Rubio-Verdú, C.; Abufager, P.; Ormaza, M.; Choi, D.-J.; Bocquet, M.-L.; Pascual, J. I.; Lorente, N.; Limot, L. Vibron-assisted spin excitation in a magnetically anisotropic molecule. *Nat. Commun.* **2020**, *11*, 1619.
(29) Kondo, J. Resistance Minimum in Dilute Magnetic Alloys. *Prog. Theor. Phys.* **1964**, *32*, 37−49.
(30) Scott, G. D.; Natelson, D. Kondo Resonances in Molecular Devices. *ACS Nano* **2010**, *4*, 3560−3579.
(31) Hellerstedt, J.; Cahlík, A.; Švec, M.; de la Torre, B.; Moro-Lagares, M.; Chutora, T.; Papoušková, B.; Zoppellaro, G.; Mutombo, P.; Ruben, M.; Zbořil, R.; Jelinek, P. On-surface structural and electronic properties of spontaneously formed Tb2Pc3 single molecule magnets. *Nanoscale* **2018**, *10*, 15553−15563.
(32) Mishra, S.; Beyer, D.; Eimre, K.; Kezilebieke, S.; Berger, R.; Gröning, O.; Pignedoli, C. A.; Müllen, K.; Liljeroth, P.; Ruffieux, P.; Feng, X.; Fasel, R. Topological frustration induces unconventional magnetism in a nanographene. *Nat. Nanotechnol.* **2020**, *15*, 22−28.
(33) Paaske, J.; Rosch, A.; Wölfle, P.; Mason, N.; Marcus, C. M.; Nygård, J. Non-equilibrium singlet−triplet Kondo effect in carbon nanotubes. *Nat. Phys.* **2006**, *2*, 460−464.
(34) Ternes, M. Spin excitations and correlations in scanning tunneling spectroscopy. *New J. Phys.* **2015**, *17*, 063016.
(35) Jacob, D.; Ortiz, R.; Fernández-Rossier, J. Renormalization of spin excitations and Kondo effect in open-shell nanographenes. *Phys. Rev. B* **2021**, *104*, 075404.

https://doi.org/10.1021/acs.jpclett.3c02401
J. Phys. Chem. Lett. 2023, 14, 11506−11512